Experimental evidence of the Non-local Response of Transport to Peripheral Perturbations

H J Sun[1,2,4], P H Diamond[1,3], Z B Shi[2], C Y Chen[2], L H Yao[2], X T Ding[2], B B Feng[2], X L Huang[2], , J Zhou[2], X M Song[2], the HL-2A[2]

[1]WCI Center for Fusion Theory, National Fusion Research Institute, Daejeon 305-806, Korea
[2] SouthWestern Institute of Physics, Chengdu 610041, China
[3] Center for Astrophysics and Space Sciences and CMTFO and Department of Physics, University of California at San Diego, La Jolla, CA 92093-0424, USA

Email: asufish@gmail.com

Abstract:

Qualitatively novel results on nonlocality phenomena in perturbative transport experiments are reported. Here, nonlocality means a rapid response in the core follows an edge perturbation on a time scale far shorter than any standard approximation to the global, diffusive model confinement time. Sequential firing of SMBI on the HL-2A tokamak sustained the increase in the core temperature in response to the edge perturbation. O-mode reflectometers are introduced to measure density fluctuations and show that the central turbulence is suppressed during nonlocallity, suggesting that the interpretation of the phenomenon as due to the formation of an 'ITB-like' structure is plausible. ECH switch-off experiments on the HL-2A tokamak demonstrated that the non-local response is sensitive to the deposition location. Taken together, these results suggest that non-locality phenomena have several aspects in common which can be linked to certain simple, generic elements of tokamak turbulence physics.

PACS numbers**:** 52.25.Fi, 52.50.Gj

1. Introduction

Phenomena suggesting fast, apparently "non-local" responses of core plasma parameters to edge perturbations have been observed in many tokamak experiments. The observation of an unusual fast heat pulse generated by the L–H transition in JET [1, 2] was the first clear non-local transport response. There are two unusual features of this heat pulse: a very fast propagation (within 1 msec) of the temperature rise and the observation that heat pulse amplitude doesn't decay in the core. Then later, the 'prompt' responses to ECRH have been observed in W7-AS [3]. In these cases, the core electron temperature responses were of the same polarity as the changes in edge electron temperature. The most striking evidence for non-locality is from cold pulses experiments, in which a transient core *Te* rise is observed in response to peripheral cooling. From the first observation of the effect at TEXT in 1995 [4] to subsequent reports on many other tokamaks and a helical device [5, 6, 7, 8, 9, 10], non-local responses induced by edge cold pulses have puzzled scientists who focus on plasma transport. This phenomenon is charactered by a simple but challenging picture: a strong cooling in the edge plasma induces significant heating in the central plasma on a timescale much shorter than a diffusive propagation time scale. This opposite response of the plasma core occurs before the edge cooling pulse reaches the central region of the plasma. Since this extremely fast response is a formidable challenge to standard transport models, the development of an understanding of the non-local effect could lead to significant new directions in research on anomalous transport.

The initial observation of nonlocal response to abrupt plasma edge cooling was performed by Gentle et al on TEXT [4]. A finite but small injection of carbon into the TEXT tokamak edge induces significant temperature perturbations throughout the plasma. Large, rapid temperature decreases are observed in the outer third, while temperatures in the inner third promptly begin to rise. The effects cannot be reproduced with transport coefficients that are functions only of local thermodynamic

variables. Later in the RTP plasmas [6, 8], a transient rise of the core electron temperature was observed when hydrogen pellets were injected tangentially to induce fast cooling of the peripheral region. The results show that the *Te* rise is associated with the formation of large temperature gradients in the region $1 < q < 2$. This region acts as a layer of transiently increased thermal resistivity (i.e.- a type of transport barrier) when probed by fast heat pulses from modulated electron cyclotron heating. Nonlocal response has been confirmed in Tore Supra by impurity injection and oblique pellet injection [7] and in the ASDEX-U tokamak [10] with laser blow-off impurity injection. Observations of nonlocal response in the LHD experiment with edge cooling suggest that the mechanism governing the nonlocality is unlikely to be linked to plasma current profile effects. However, despite the experimental progress, the mechanism of nonlocal response in the edge cooling experiment remains unclear.

Non-locality experiments present several challenging questions, which include but are not limited to:

i) Are non-local responses really non-local or simply fast, relative to conventionally quoted transport time scales?

ii) What physics sets the fast time scale and determines the response dynamics? In many cases, the core responds after only 1 msec, while transport time scales are around 30-50 msec. Indeed, such a fast time response suggests that mesoscale or microscale processes must be conflated with macroscopics to form the non-local response.

iii) What is the relation of the fast non-local response to the physics of profile structure formation and evolution? In this vein, the similarity of cold pulse induced transient rise in central temperature (and the steepening of ∇T_e outside the $q = 1$ surface) to ITB formation has been suggested [8]. In the usual case, the steepening of profile by an ITB will be sustained until instabilities driven by the steepened gradient (i.e. ELMs, MHD) destroy the ITB. In nonlocality, the steepening is sustained about one energy confinement time, so the ITB-like structure decays by transport. However, on HL-2A, sequential SMBI can be used to sustain the steepening of

temperature profile significantly longer, i.e. for several confinement times. This method is difficult to use continuously, since the increase of core temperature will stop once the density exceeds the cutoff density for nonlocality, which is inevitable because of sequential SMBI.

In this article, we will report several new experimental results on non-local transport phenomenon induced by various triggering methods performed in the HL-2A. The different techniques which were used to induce edge Te perturbation to study nonlocal response are summarized in Table 1. Supersonic molecular beam injection (SMBI) has been well developed as a repetitive refueling peripheral perturbation method on HL-2A. It is possible to study non-local response to different edge perturbation rates by control SMBI size and duration and the modulated SMBI can be used to trigger repetitive non-local response (section 3.1). Some new results for density fluctuation measured by reflectometers will be introduced in this section. As a complementary method of SMBI, far off-axis ECRH switch-off will provide a precise analysis of how initial perturbative position affects non-local response (section 3.2). A comparison of results by different triggers and discussion is given in section 4 and a summary is presented in the last section.

Table 1 the features and advantages of various methods which are introduced to study nonlocality in this paper

method	Features and Advantages
SMBI	Flexibility of perturbation rate, sequential firing to trigger repetitive nonlocality and sustain the steepening of the temperature profile.
ECRH switch-off	Well-localized, to provide a precise analysis of initial perturbation

2. Experimental setup

HL-2A is a diverted tokamak (major radius R = 1.65 m; minor radius a < 0.40 m) which can be operated in either a limiter or single null-divertor configuration. It has the following parameters: toroidal magnetic field Bt < 2.8 T, the line average electron density ne = *(*0.5–5*)* × 10^{19} m^{-3} plasma current Ip < 350 kA [11]. Figure 1 shows the

experimental setup of the SMBI system on HL-2A. The SMBs are driven by a magnetic-electric valve and can be injected from both the low field side (LFS) and the high field side (HFS) [12]. With a pressure of 0.2–3MPa and duration of 1–10 ms, up to 50 SMBs can be injected from the LFS, thus introducing a new modulation method with which to investigate electron heat transport. More than 30 diagnostics have been deployed on HL-2A in recent years. Among them, the key diagnostic for this experiment is the ECE diagnostic. Two ECE systems have been installed on HL-2A: one a scanning heterodyne radiometer and the other a fast multichannel ECE system. An introduction to the scanning heterodyne ECE can be found in [13]. The fast ECE system includes 16 channels, and the RF range is between 110 and 130 GHz, with a bandwidth of ~1.5 GHz. For the standard discharge parameters (Bt ~ 2.4 T) in HL-2A, the heterodyne radiometer can provide a complete electron temperature profile with a temporal resolution of 4ms and a spatial resolution of 4 cm. The fast multi-channel ECE system could be utilized to measure the temperature perturbation with certain good temporal resolution of 1μs and the spatial resolution of around 3 cm. For some particular physics experiments, low parameters (Bt ~ 1.2–1.45 T) are necessary. In that case, the fast ECE will provide the electron temperature by changing the LO and the mixer.

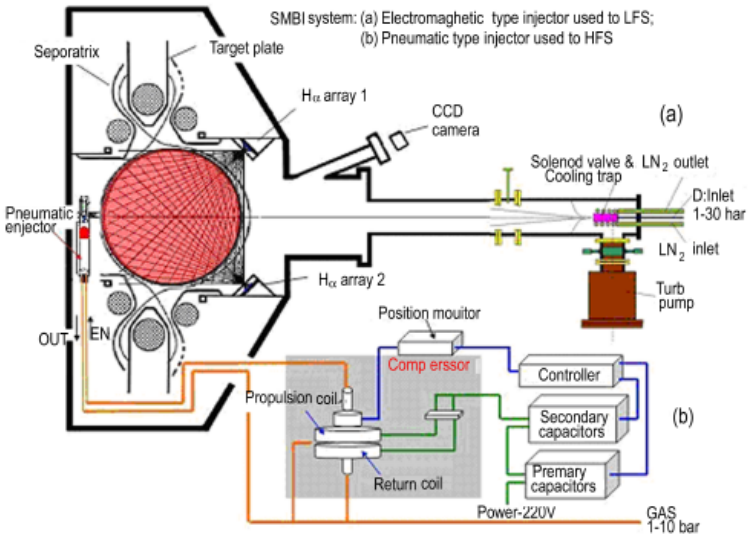

Figure 1 the experimental set-up of SMBI system on the HL-2A tokamak

3. Experimental results

3.1 Sustained Nonlocal Response induced by SMBI on HL-2A

For density lower than 2×10^{19} m^{-3}, a transient rise of the core electron temperature has been observed when repetitive SMBs are injected to induce fast cooling of the peripheral region ($\rho \geq 0.7$), as shown in figure 2. The core temperature rise has strong density dependence: it is more than 600 eV when the electron density n_e is around 0.7×10^{19} m^{-3}, it decreases to 150 eV when n_e is around 1.36×10^{19} m^{-3} and disappears when n_e is larger than 1.5×10^{19} m^{-3}. This cut-off density is close to the critical density at which the Ohmic L-mode energy confinement changes from the linear to the saturated regime on HL-2A. The cutoff density of reflectometer for density profile on HL-2A is around 0.8--2×10^{19} m^{-3}, so there is no density profile for usual nonlocality experiment. But with higher parameters and high ECRH heating power, the cutoff density for nonlocality can be increased [14]. In shot 15764, nonlocal response was triggered by SMBI with higher line averaged density (2×10^{19} m^{-3}). A steeper temperature profile is observed after the non-local response effect appears, while there is no obvious change in density gradient, as shown in figure 3. Usually the duration of the central Te rise is about 30 ms, which is roughly comparable with the energy confinement time τ_E on HL-2A. Sequential firing of the SMBI can effectively sustain the increased core temperature, which appears to follow in response to the edge perturbation, as shown in figure 4. The duration of sustainment is four times longer than the confinement time τ_E. Both the bolometer radiation and the Hα emission decrease when the core T_e increases, accompanied by the increase of the stored energy. Obviously, the duration of improved confinement plasma is prolonged along with the duration of the increased core T_e rise. The delay time of the response of the plasma center to the edge perturbation, defined as the delay of the initial central temperature rise relative to the initial time of the edge temperature drop, is around 1 ms, seen in figure 4b. The perturbation reversal position

is outside the $q = 1$ surface, as determined from the inversion radius of sawteeth oscillations and EFIT calculation.

Another interesting phenomenon was found during nonlocal experiments, namely a propagating heat pulse originating from the central temperature rise arrives at the outer region, sometime after the cold pulse induced by SMBI, as shown in figure 5. Here, no evidence for the presence of a significant shift of the plasma column induced by the cold pulse is observed by the magnetic measurement system. This usually happens in ECRH regimes, i.e. higher electron temperature plasma.

The O-mode reflectometers are introduced to measure density fluctuation. Figure 6 and figure 7 show the spectrum evolutions of the density fluctuations with sequential SMBI, which is measured by 27GHz or 35GHz reflectometer. In fugure 8, repetitive non-local effect has been triggered by SMBI, while no nonlocality appears in figure 9 because the density is higher. In figure 6, the line averaged density is about (0.8-1.1)*$10^{19}$$m^{-3}$, the cutoff surface of 27 GHz is estimated at *r/a* = 0.3-0.5 The central turbulence is suppressed after SMBI during non-local effect. In figure 7, the line averaged density is around 1.5×10^{19} m^{-3} and from the ECE temperature signal, there is no rise in central temperature after SMBI. The central turbulence increased after SMBI in this case. This suggests that the steepening of core ∇Te and the rise in the central temperature are due to a local reduction in turbulence and the associated transport. This observation suggests the interpretation of the non-locality as one where the edge perturbation includes a global change in temperature profile morphology ITB to a state which resembles that of an ITB.

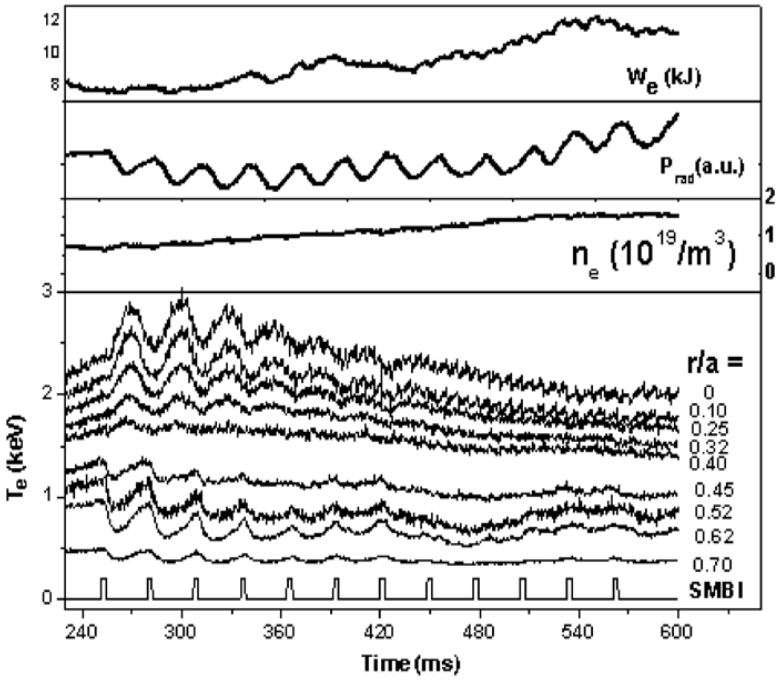

Figure. 2 Evolution of parameters in shot 8363 with SMBI. From top to bottom: the storage energy *W*e, the bolometer signal, the electron density, ECE temperature at different radii and the SMBI signal in the ohmic regime (*B*t = 1.45 T, *n*e = (0.7–1.5) × 10^{19} m^{-3}, *I*p = 190 kA). The nonlocal response of central plasma becomes weaker as the density increases and finally disappears when the density is around 1.5×10^{19} m^{-3} (cut-off value).

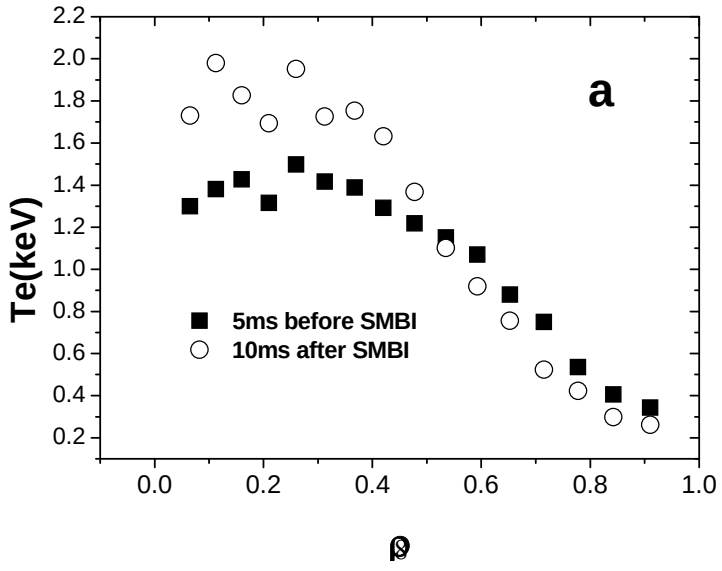

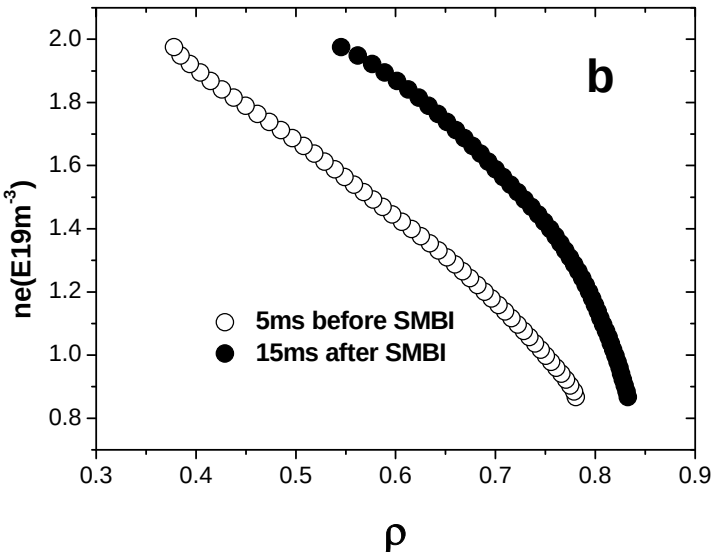

Figure 3. a) temperature profile evolution during a non-local effect induced by SMBI by ECE measurement, b) density profile evolution during nonlocality by microwave reflectometer. The temperature gradient becomes steeper, while there is no obvious change in density gradient.

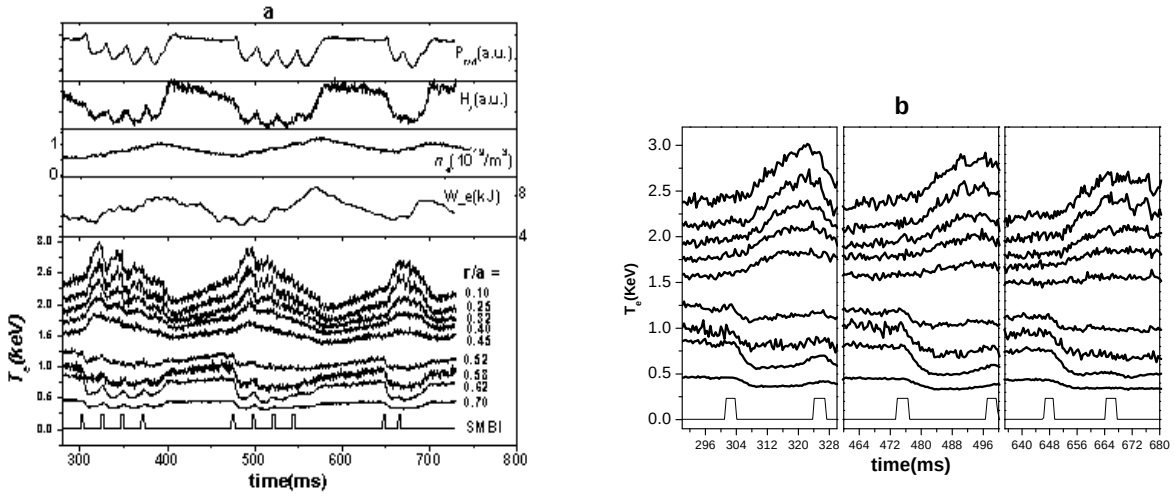

Figure 4 (a) Parameters evolution in shot 8364 with SMBI. From top to bottom: the bolometer signal, the Ha signal, the electron density, the stored energy W_e, ECE temperature at different radii and the SMBI signal in the ohmic regime.(B_t = 1.45 T, n_e = 0.6 – 1.2×10^{19} m^{-3}, I_p = 190kA.) (b) The delay of the initial central temperature rise

relative to the initial edge temperature drop. The increased core temperature has been sustained by sequential firing of the SMBI. The duration of sustainment is more than three times longer than the confinement time τ_E .

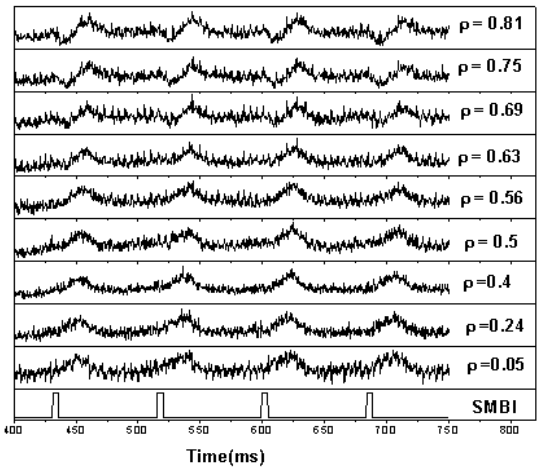

Figure 5 Shot 13125, experimental time traces of electron temperature for periodic SMBI. Propagating heat pulses originating from the central temperature rise arrive at the outer region, sometime after the cold pulse induced by SMBI.

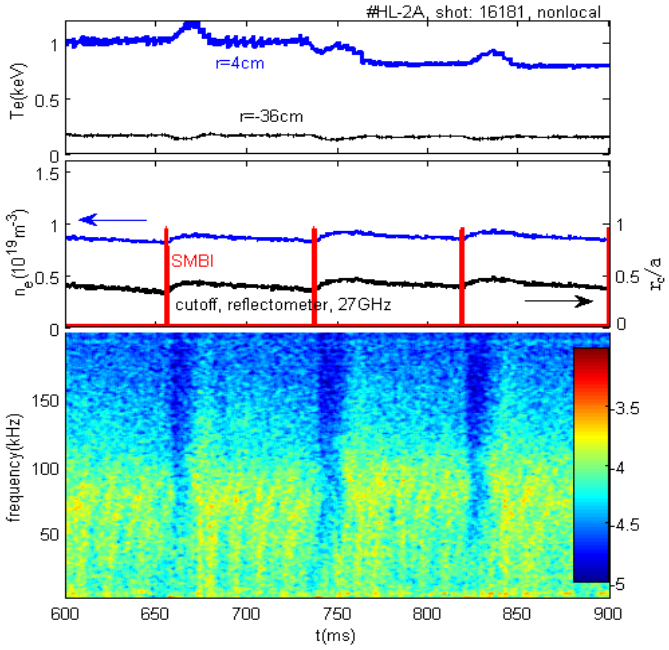

Figure 6 shot 16181, sequential SMBI induces nonlocal effect. From top to bottom: the core and edge Te, line averaged density and cutoff surface of reflectometer, power spectrum of density fluctuation. Power spectrum shows the central turbulence suppression during nonlocal effect measured by 27GHz reflectometer.

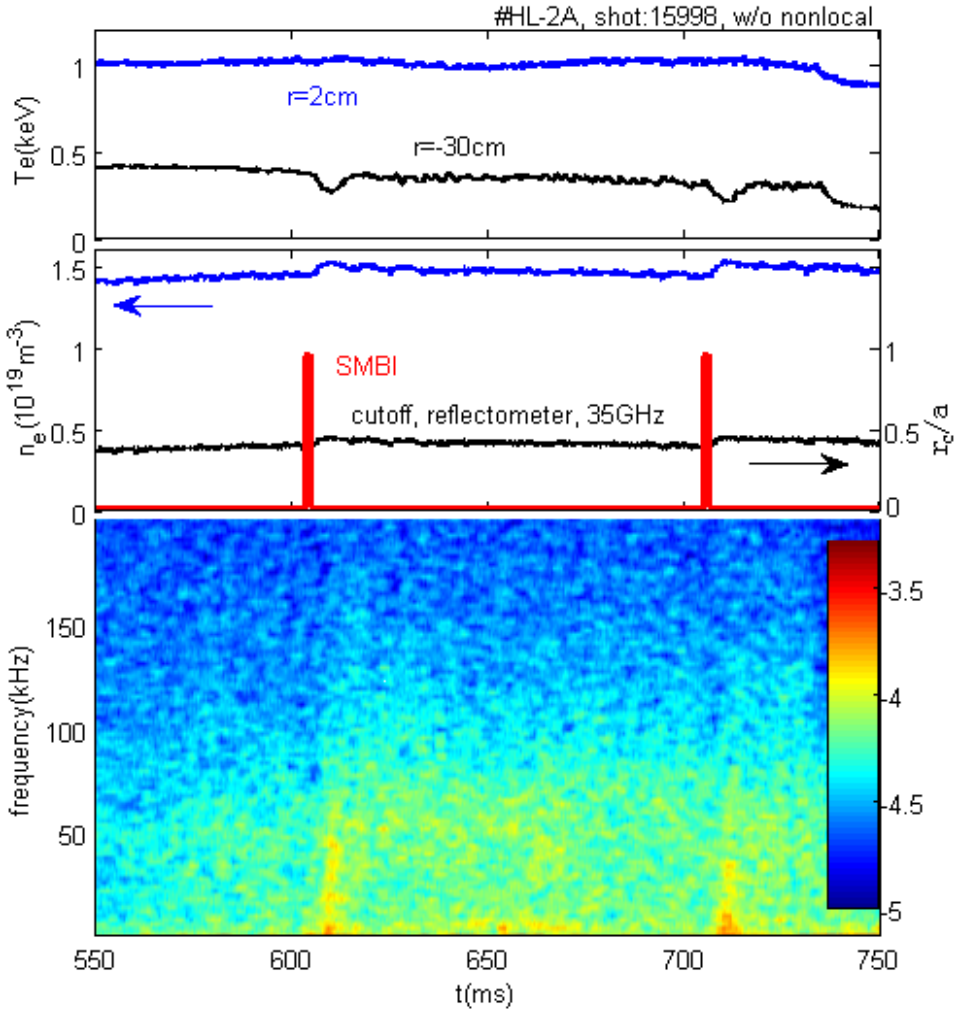

Figure 7 shot 15998, normal cold pulses induced by SMBI, without nonlocal effect. From top to bottom: the core and edge Te, line averaged density and cutoff surface of reflectometer, power spectrum of density fluctuation. Power spectrum shows the increase of the central turbulence after SMBI

3.2 Off-axis ECRH switch-off

In addition to normal cold pulse injection (i.e. Pellet injection, SMBI, impurity injection, etc), far off-axis ECRH switch-off can be also used to create inward cold pulse propagation. One would expect similar non-local effects with the edge cooling by off-axis ECRH switch-off. This was tested on HL-2A in experiments with various ECRH depositions by scanning the toroidal magnetic field. When the power deposition was moved to plasma edge ($\rho \approx 0.7$) after the off-axis ECRH switch off, the core electron temperature did not decrease immediately. Instead, the core temperature increased for several tens of milliseconds before it started to decrease. In contrast, the edge temperature decreased just after the ECRH switch off, as shown in figure 8. This phenomenon is quite similar to the non-local effect induced by SMBI. Here, the core response appears more slowly than the usual cold pulse case, and the time delay is several msec.

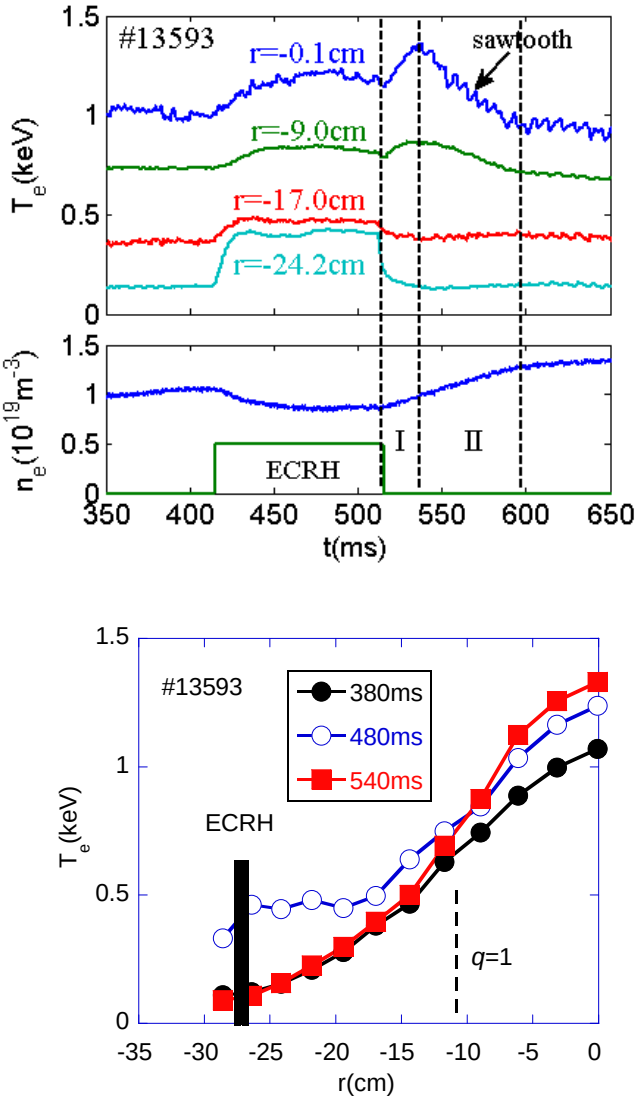

Figure 8. (a) Time evolution of the electron temperature and density after ECRH switch-off (at 515 ms) (shot#13593, B_t=1.42 T, I_p=170 kA, P_{ECRH}=740 kW). The ECRH resonance is at 27.8cm ($r_{dep}/a \sim 0.69$); (b) Temperature profiles at 380 ms, 480 ms and 540 m. The core temperature increases after ECRH switch-off and the temperature profile becomes steeper in the reverval radius.

Figure 9 shows the power spectra of the density fluctuations of the same discharge in figure 8 which is measured by 35GHz reflectometer before (380 ms), during (480 ms) and 25 ms after (540 ms) ECRH. The cutoff surface is estimated to be located at r/a = 0.1-0.5 in this shot since the line averaged density is about (1-1.4)*$10^{19}m^{-3}$. The power spectrum after ECRH switch-off is much lower than that before or during ECRH. This suggests that the central turbulence is suppressed after ECRH is turned off.

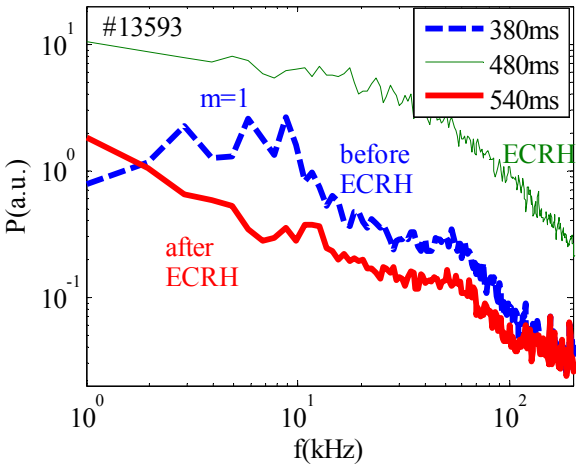

Figure 9 power spectrum showing the turbulence suppression after ECRH switch-off. The ECRH power deposited at 27.8cm (r_{dep}/a ~0.7).

4. Summary and Experimental Analysis

Experiments using SMBI and off-axis ECRH switch-off as peripheral cooling methods in the HL-2A tokamak confirm and extend the observations of nonlocality made in other machines. Sequential firing of the SMBI can effectively sustain the increased core temperature which appears to follow in response to the edge perturbation. The period of central temperature increase can be extended to several global energy confinement times by repetitive SMBI. The duration of the core temperature increase can be prolonged until the density reaches the nonlocal cut-off density for nonlocal phenomena. The central turbulence is suppressed perturbation induced steepening of ∇T suggesting that the interpretation of the phenomenon as 'ITB-like' is plausible. When the edge perturbation becomes stronger, the non-local response in the core also becomes stronger. Experiments on off-axis ECRH switch-off shows that the deposition location of initial perturbation is important in achieving a non-local response. On HL-2A, the deposition position of ECRH should be outside $\rho \approx 0.7$ so it can trigger non-local response. It seems like $\rho \approx 0.7$ is a 'special' location for non-local transport phenomenon. On HL-2A, the location is related to the radius of the q=2 surface.

In this section, the following questions are discussed:

i. How do the size of the edge temperature and density perturbation affect the temperature rise in the core, i.e. what is the correlation between $\delta Te(core)$, $\delta ne(core)$ and $\delta Te(edge)$?

ii. How does the initial perturbation position in the peripheral plasma affect the non-local response?

iii. What are the possible physics mechanisms related to the response in the core? In particular, what sets the time scale? Also, what sets the inversion location?

SMBI experiments have been carried out to determine the correlation between the edge perturbation and core perturbation on HL-2A. A nearly linear relation between the edge perturbation ($\rho \approx 0.7$) in both density and temperature and the central temperature rise ($\rho \approx 0.1$) has been observed, as shown in figure 10. When the edge perturbation becomes stronger, the non-local response in the core also becomes stronger.

The relative amplitudes of the central response are plotted versus the corresponding ECRH deposition position in Figure 11. The change of the central temperature 20 ms after ECRH switch-off is compared to the moment before switch-off. In the case of on-axis or nearly off-axis ECRH (inside q=1 surface) switch-off, the central temperature usually drops back to the amplitude it had prior to application of ECRH. In the case of far off-axis ECRH ($\rho \approx 0.7$), a non-local rise on the core temperature was observed. According to the EFIT estimation, the deposition position is outside the q=2 surface. But a delayed drop of the central temperature is observed if the ECRH deposition is between q = 1.0-2.0, as is similar to the observations in T-10 and TEXTOR tokamaks [15, 16]. The delayed drop of the central temperature becomes strong when the ECRH deposition position moves from center to edge. A detailed study of the delayed drop with ECRH switch-off can be found in [15, 16] and references therein. So if one expects the observation of non-local response in the core plasma, the perturbation position should be put at radii with

$\rho > 0.7$.

According to the temperature profile evolution in figure 3 and 8, one may suggest that the formation of a structure similar to an electron internal barrier (ITB) [8] is what causes the suppression of core turbulent transport. Caution is required, however if the ITBs are weak, they may be destroyed by the inward cold pulse, ending to a final outward-travelling heat pulse (see figure 7). Also, the physics of this 'ITB' formation is not clear, so more efforts should be devoted to its study.

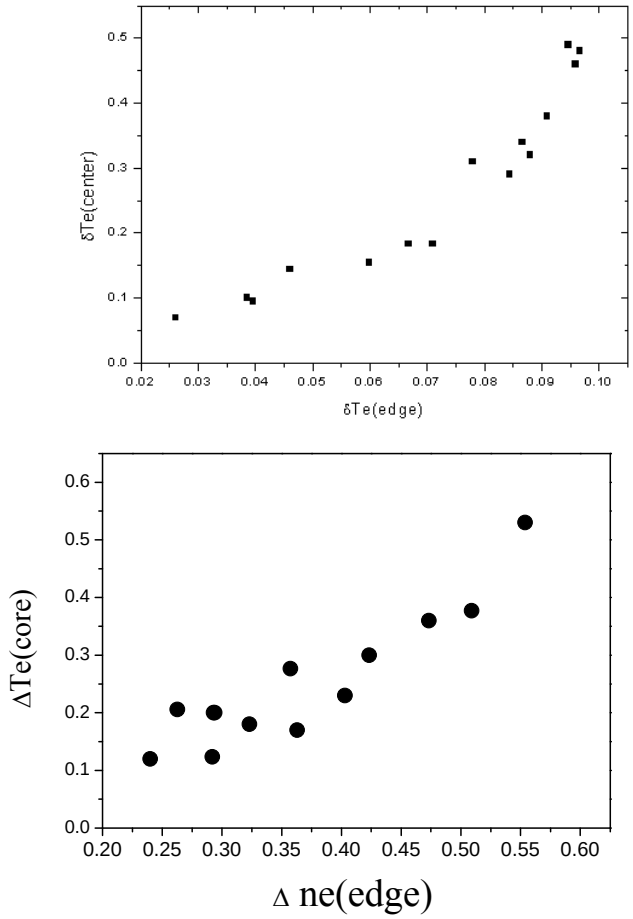

Figure 10 The relation between edge temperature cooling a) and edge density perturbation b) and center rise during non-local effect. A nearly linear relation between the edge perturbation ($\rho \approx 0.7$) in both density and temperature and the central temperature rise ($\rho \approx 0.1$) has been observed,

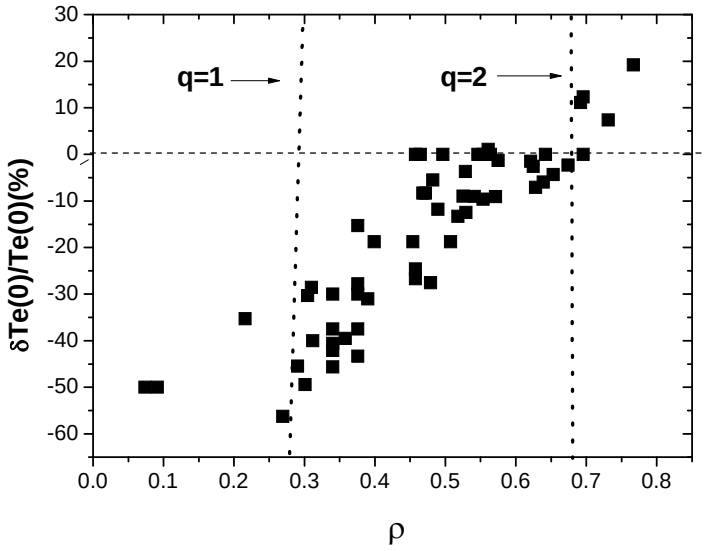

Fig. 11. Relative central temperature change in the timescales of 20 ms after ECRH switch off. a delayed drop of the central temperature is observed if the ECRH deposition is between q = 1.0-2.0. In the case of far off-axis ECRH ($\rho \approx 0.7$), a non-local rise on the core temperature was observed

5. Discussion

Taken together, the results of cold pulse and nonlocality experiments present an interesting but formidable challenge to our understanding of turbulent transport phenomena and profile self-organization in magnetic confinement devices. In this section, we discuss:

i.) the principal experimental findings which a theory of cold pulse non-locality experiments must address.

ii.) aspect of mesoscale fluctuation and self-organization dynamics which are useful in confronting the issues listed in (i).

iii.) a critical evolution of how the theory has performed when compared to experimental results.

iv.) some thoughts on promising directions for future work.

We emphasize here that this discussion is not a review, which is beyond the scope of this paper. Rather it is offered as a critical assessment of the current status of the theory. Readers seeking a comprehensive overview should consult the review article by Callen [17]. Here, we focus on the theme of the implications of cold pulse experiments for mesoscale self-organization processes.

The cold pulse experiments, including those discussed in this paper, present several unresolved puzzles. These include, but are not limited to:

i.) the fast response issue —i.e. how does edge cooling provoke central heating on a time scale more than an order of magnitude shorter than the global energy confinement time [4-10] (i.e. for HL-2A, discussed here, ~ 1 msec vs ~ 30 msec).

ii.) the temperature gradient steepening or transient ITB formation at the inversion radius — i.e. how does the edge cooling provoke an apparent change in transport state, or transport bifurcation? This phenomenon strongly suggests the existence of a feedback loop which links the edge perturbation response to the profile structure. A related question concerns what sets the location of the inversion or transient ITB.

iii.) the results of fluctuation measurements presented in this paper that indicate a drop in turbulence in regions of ∇T steepening. This observation re-inforces the notion that the response to the cold pulse triggers the formation of what may be thought of as a transient ITB state.

iv.) the possibility to sustain the 'transient ITB' state for multiple energy confinement times (i.e. up to $4\tau_E$) by repetitive SMBI (figure 4). This remarkable result suggests that what we have been calling 'nonlocality events' are, indeed, better thought of as global changes in profile morphology induced by edge perturbations. This new profile morphology is seemingly meta-stable and can be sustained until the density hits the cut-off value. We note that spontaneous reversals in Ohmic plasma intrinsic rotation [18, 19] are another example of large scale profile morphology changes induced by small perturbation — in that case by increasing the density to the onset level for Ohmic confinement saturation. Another is the novel tokamak state with global stationary temperature oscillations discovered by Giruzzi, et al [20]. All of these phenomena are suggestive of a sort of transport bifurcation, leading to a metastable transport barrier-like state.

v.) the existence of a cut-off density n_{crit}, such that for $n > n_{crit}$, electron temperature non-localtiy is not observed. In many cases, n_{crit} is a substantial fraction of the Greenwald density limit [21].

Items i–v are the main challenges the cold pulse experiments present to confined plasma.

The road to understanding 'non-locality experiments' inevitably leads us to discuss mesoscale dynamics, mesoscale ℓ_{meso} sits between the turbulence correlation length Δ_c and the system size a, such that $\Delta_c < \ell_{meso} < a$. This leaves considerable turbulence dynamic range for mesoscale structures, given that turbulence correlation lengths are rather small with $\Delta_c \sim few\ \rho_i$ and the system size is large enough that

$\rho_* \leq 10^{-2}$. Mesoscale phenomena offer the most direct and plausible alternative to purely diffusive transport mechanisms, which intrinsically can't explain the cold pulse phenomena. Thus, turbulence avalanching and spreading — a mechanism for fast radial propagation and profile modification — naturally emerges as an attractive candidate mechanism. Here, we briefly discuss the basic physics of avalanching and spreading, with the more detailed comparisons to nonlocality experiments, which follow below. Once again, we emphasize that this is not a comprehensive review article. Hence, we limit our discussion to theoretical approaches which can be reconciled with dynamics, specifically:

i.) the drive of turbulence and transport by spontaneous profile relaxation mechanisms— i.e. instabilities, though not necessarily of the linear variety.

ii.) the self-consistent formation of sheared zonal flow by the turbulence dynamics. Any credible model ultimately must include and address shear flow phenomena, since shear flows are natural 'predators' which feed off of, and retain free energy released by the underlying gradient drive. Interaction of non-locality responses with turbulence driven shear flows is a key question.

Avalanching and turbulence spreading is, to our knowledge, the only approach to non-locality phenomena which has been shown to fit into a self-consistent dynamical framework, and so here we focus on it, exclusively. Readers wanting an all-inclusive survey should consult the review [17].

We hereafter use the word 'avalanching' to describe the processes of turbulence propagation [22, 23, 24, 25] and profile evolution by gradient toppling feedback and self-scattering and entrainment (see figure 12). Though discovered or realized and usually discussed independently, profile toppling and spreading are really inseparable, though conceptually distinct, pieces of a single process, which we hereafter refer to simply as 'avalanching', Turbulence avalanches or propagates by sequential overturning of adjacent eddies or cells and by entrainment of neighboring regions by

localized turbulence excitations. In formal terms, these nonlinear processes correspond to spatial coupling by gradient evolution and to nonlinear eddy-eddy scattering, respectively. Fig 12 presents a cartoon which illustrates these processes. Avalanches may be thought of as scale independent transport events, usually with power law probability distributions [26], which nonlinearly propagate heat, particles and turbulence intensity. Avalanching is characterized by non-diffusive kinetics [27]. It originates from the spatial structure and orientation of fluctuation in confined plasma, and is observed in experiments [28] and simulations [29, 30]. Avalanching has been shown to induce an effectively non-local thermal conductivity [31].

Shear flows, including zonal flows [32], are generated by turbulent Reynolds stresses driven by fluctuations and thus necessarily are tightly couples to the avalanche dynamics by a predator—prey type feedback loop. In particular, states of strong shear flow and strong avalanching may tend toward mutual exclusivity. More generally, the question of how the system solves the pattern selection problem of avalanches vs zonal flows looms as an important one here. One possibility is a spatial decomposition, into a quasi-regularly spaced staircase of shear layers with zones of avalanching located in between. This type of structure has been observed in simulations [31]. An alternative is a cyclic state of alternating time periods dominated by zonal flows and avalanches respectively. It is fair to say that the pattern selection struggle between shear flows and avalanches remains rather poorly understood. It is a crucial question, though, since strong shear flows can be expected to inhibit fast radial propagation.

We now come to the principal focus of this section, which is how well avalanching models of the plasma response to cold pulse perturbations perform upon comparison to experimental results. We consider the five principal unresolved puzzles, discussed above

i.) regarding the fast response issue, avalanching and turbulence spreading offer a promising route towards an explanation of the short response times observed in nonlocality experiments. Avalanching and turbulence

spreading —i.e. propagation of a turbulence front— are due to mode-mode scattering in k and position space [22-24, 27, 33-35]. Simple models of turbulence spreading using reaction-diffusion methods suggests that a turbulence front propagates ballistically at the speed $V \sim (D\gamma)^{1/2}$, (the Fisher velocity) where D is the local mean turbulent diffusivity and γ is the local turbulence growth rate. Taking $D \sim \rho_*^{\alpha} D_B$ and $\gamma \sim V_{Thi} / L_{\perp}$ (here D_B is Bohm diffusivity, $\rho_* = \rho_i / L_{\perp}$. $\alpha = 1$ for Gyro-Bohm diffusion scaling, while $\alpha = 0$ for Bohm scaling), gives $V \sim (\rho_*)^{(1+\alpha)/2} V_{Thi}$. Note that $\alpha = 1$ gives $V \sim V_*$ while $\alpha = 0$ gives $V \sim (\rho_*)^{1/2} V_{Thi}$, which can significantly exceed V_*. Observe that the pulse propagation speed gives a clue concerning scale length dependence of ρ_*, through the α dependence of V. Also note that a turbulence front is necessarily part of any radial avalanche propagation process. Using the typical parameters for HL-2A shown in figure 2 (B_t = 1.45 T, T_e = 1 KeV) and using the gradient change at the position $\rho \approx 0.7$ for the same shot as L_T^{-1}, V_* is of order of 1-2 Km/s, at which speed a cold pulse propagate from edge to center within 1 ms. Finally, we comment that the Fisher speed $V \sim (D\gamma)^{1/2}$ is a plausible answer to the ever-present question of "how can non-diffusive, ballistic dynamics emerge from a basically diffusive transport?" Thus, we see that the avalanching and spreading models offer a plausible explanation of the fast response times observed in cold pulse experiments.

ii.) Regarding the transient 'ITB' and inversion issue, none of the avalanching theories have yet been systematically applied to the modeling of cold pulse experiments. The crucial question of course is whether the model contains a sufficient strong feedback loop so a

transient gradient steepening is possible. In general, the question of feedback loops has not received sufficient attention in the context of explaining non-locality experiments. Candidate feedback loop mechanisms include, but are not limited to, $\vec{E} \times \vec{B}$ shear and profile dependence of the instability threshold function. Preliminary results [36] from the model of ref [35] indicate that self-consistent $\vec{E} \times \vec{B}$ shear suppression can allow sufficiently strong gradient feedback so as to trigger a transient gradient steepening and inversion. It is important to note here that much more work is required to determine if this scenario can survive a quantitative confrontation with the experimental results.

iii.) Regarding fluctuation measurements, it is fair to say that any feedback loop which yields ∇T_e steepening must also predict a reduction in fluctuation intensity, since electron thermal transport is fluctuation driven. Thus, the fluctuation response is tightly linked to the feedback loop issue (ii) above. The real question in fluctuations is quantitative — how much of a reduction in fluctuations is predicted and how is it related to the increase in ∇T. No theoretical modeling effort has yet confronted this question.

iv.) Regarding the repetitive SMBI experiments, theoretical models have not yet been applied to these interesting results. Work on this question is ongoing.

v.) The physics of the cut-off density remains a mystery. One interesting possibility is that the cut-off is symptomatic of the thermal coupling to the ions, so $n_{cut\text{-}off}$ should be related to the n_T, the value of density at which the linear Ohmic confinement saturates. Since the cold pulse induces a local perturbation, $n_{cut\text{-}off}$ may be related to n_T but not identical to it. One signature of this speculation would be a fast transient in the core ion thermal channel in response to a cold pulse at $n \sim n_{cut-off}$. We

are not aware of any which supports this speculation, but neither are we aware of any studies which addressed the ion thermal response to the cold pulse.

All told, it seems fair to say that self-consistent theoretical modeling is only beginning to confront many of the challenges in nonlocality experiments and that much further work is required. Perturbatively triggered feedback loops appear to be the major unknown.

Finally, we also comment here that the theoretical perspective discussed above and presented in detail in Reference [35] needs considerable further development in order to quantitatively address these nonlocality phenomena. Distributed Ohmic heating (set by the q(r) profile) and collisional electron heat coupling to ions cause a departure of the Ohmic transport from the "fixed flux" formulation beloved by theorists. A density evolution equation, with a particle pinch term, should be added. The turbulence model should probably be based on TEM (Trapped Electron Mode) ---- and likely DTEM (Dissipative Trapped Electron Mode) or weak CTEM (Collisionless Trapped Electron Mode) ---- with drive by both ∇T and ∇n. A separate T_i evolution equation is required to properly treat evolution of the diamagnetic $\vec{E} \times \vec{B}$ shear. We note in passing that given the global, strongly nonlinear character of these phenomena, they will likely remain intractable for gyrokinetic simulation until sometime considerably in the future. Thus, there really is no alternative to the reduced models described here.

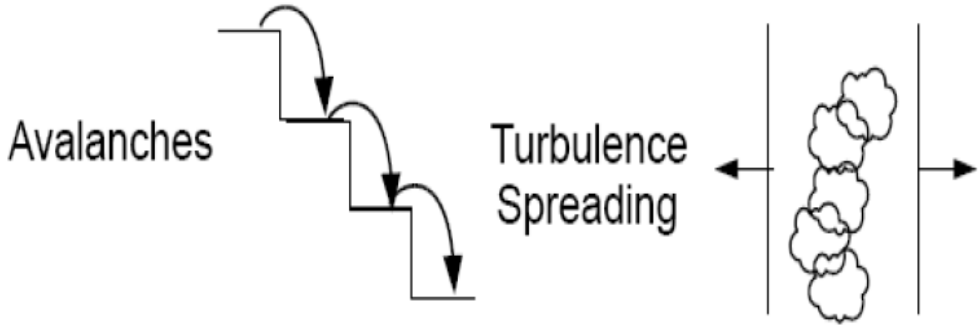

Figure 12: Schematic plot of avalanches (left) and turbulence spreading (right)

Acknowledgments

We thank Zhanhui Wang, Jiaqi Dong, P. Mantica, X. Garbet and X L Zou for useful discussions. This work was supported by the National Science Foundation of China under grant No. 10975049 and No. 11005037. This work was supported by the World Class Institute(WCI) Program of the National Research Foundation of Korea(NRF) funded by the Ministry of Education, Science and Technology of Korea(MEST) (NRF Grant Number: WCI 2009-001).

References

[1] Neudachin et al 20th EPS conference on controlled Fusion and plasma physics, Lisbon, 1993, volume 17C, part I, P.83 (1993).
[2] Cordey J G *et al* 1994 *Plasma Phys. Control. Fusion* **36** A267
[3] Stroth U *et al* 1996 *Plasma Phys. Control. Fusion* **38** 611
[4] Gentle K W et al 1995 *Phys. Rev. Lett.* **74** 3620.
[5] Kissick M W et al 1998 *Nucl. Fus.* **38** 821.
[6] Hogeweij G M D et al 2000 *Plasma Phys .Contr. Fusion* **42** 1137.
[7] Zou X L et al 2000 *Plasma Phys. Control. Fusion* **42** 1067.
[8] Mantica P et al 1999 *Phys. Rev. Lett*. **82** 5048.
[9] Tamura N et al 2007 *Nucl. Fus.* **47** 449
[10] Ryter F et al 2000 *Nucl. Fus.* **40** 1917
[11] Yang Q W et al 2007 *Nucl. Fus.* **47** S635
[12] Yao L H et al 2007 *Nucl. Fus.* **47** 1399
[13] Shi Z B et al 2005 *Plasma Phys .Contr. Fusion* **47** 2019
[14] Sun H J et al 2008 *Chin. Phys.Lett* **24** 2621
[15] Hogeweij G. M. D., et al. 1998, Nucl. Fusion, **38**, 1881.
[16] Razumova K. A., et al. 2004, *Nucl. Fusion*, **44**, 1067.
[17] Callen J D and Kissick M W 1997 *Plasma Phys .Contr. Fusion* **39** B173
[18] Bortolon A et al 2006 *Phys. Rev. Lett*. **97** 235003.
[19] Rice J. E et al. 2011 'Rotation Reversal Bifurcation and Energy Confinement

Saturation in Tokamak Ohmic L-mode Plasmas' *Phys. Rev. Lett*. (submitted)
[20] Giruzzi G et al 2003 Phys. Rev. Lett. **91** 135001
[21] Greenwald M 2002 *Plasma Phys. Control. Fusion* **44** R27
[22] Garbet X, Laurent L, Samain A and Chinardet J 1994 *Nucl. Fusion* **34** 963-74
[23] Hahm T S *et al* 2004 *Plasma Phys. Control. Fusion* **46** A323
[24] Gurcan O, Diamond P, Hahm T, and Lin Z, 2005 *Phys. Plasmas* **12**, 032303
[25] Naulin *et al* Phys Plasma**12**, 122306 (2005)
[26] Itoh S *et al* 2004 *Plasma Phys. Control. Fusion* **46** A341-A346
[27] Hasegawa A and Mima K 1978 *Phys. Fluids* **21** 87-92
[28] Politzer P A 2000 Phys. Rev. Lett **84** 1192-95
[29] Sarazin Y *et al* 2010 *Nucl. Fusion* **50** 054004
[30] Idomura Y *et al* 2009 *Nucl. Fusion* **49** 065029
[31] Dif-Pradalier G et al 2010 *Phys. Rev. E* 82 025401-4
[32] Diamond P H *et al* 2005 *Plasma Phys. Control. Fusion* **47** R35
[33] Diamond P. H. and T. S. Hahm, 1995 Phys. Plasmas **2**, 3640
[34] Garbet X, Sarazin Y, Imbeaux F, Ghendrih P, Bourdelle C, Gürcan Ö D and Diamond P H 2007 *Phys. Plasmas* **14** 122305
[35] Wang Z H and Diamond P H *et al* 2011 *Nucl. Fusion* **51** 073009
[36] Diamond P.H. *et al* 2011 1st Asia Pacific Transport Working Group (APTWG) International Conference *(Gifu, Japan, 2011)* B-O1 and *http://peras.nifs.ac.jp/aptwg2011/center*